

VI. Immiscible fluids

We shall continue our study of real fluids with an interesting phenomenon that is strangely absent from some textbooks on thermodynamics and the main subject in others. Here, in the first place, we shall introduce interactions between the components of a **mixture**. After all, the form of the free energy of a real, pure gas reflects the influence that each particle has on its neighbors; so it is reasonable to expect that unlike particles also interact with each other.

VI.1. Ideal gases with mutual interaction

When 2 fluids are mixed, and afforded enough time to settle down, one of two things may happen. (1) The system approaches an equilibrium state in which the mixture is uniform, the concentration $\rho_1/(\rho_1 + \rho_2)$ having the same value throughout the vessel. Such mixtures are said to be **miscible**. (2) But sometimes the two fluids may not mix so readily. A small amount of each fluid can be dissolved in the other, either way, within limits. But at a range of temperature and pressure, if the average concentration is too high, then a different type of equilibrium may be observed, typically containing bubbles of one fluid mixture floating in a background of another fluid mixture with very different concentration. Because this chaotic configuration, with variable droplet size and a major influence of surface tension, is difficult to analyze, let us admit the presence of the standard gravitational field. Then a likely result is that the heavier fluid occupies the lower part of the vessel (a small amount of the lighter fluid dissolved in it) while the lighter fluid occupies the rest (a small amount of the heavier fluid dissolved in it).

Examples involving two liquids, a liquid and a gas or a gas and a solid are common, but it is reported that the combination of any pair of ‘gases’ is completely miscible.¹ The processes by which such things may come about are almost beyond analysis, but we can try to understand the final, equilibrium states. The role of gravity is not taken into account quantitatively. Gravitation is used only to explain the observation that the fluid separates into distinct regions with smooth boundaries and our studies concern the final, equilibrium configurations.

In the case of two fluids of very different nature the Dalton law of partial pressures is not expected to be valid, and the strong Gibbs-Dalton hypothesis must at least be modified, see Section V.5. One expects that there is an interaction between two dissimilar atoms. As before, in section 5.6.1, we add a van der Waals interaction term to the free energy. Because we are interested in the equilibrium states the density gradients will be small and it is enough to consider an **interaction energy** that is an algebraic function of the densities, not involving their gradients. We shall include the following term in the free energy density of the mixture of two ideal gases,

¹This is what we read in many places, but if a van der Waals fluid above the critical point is ‘a gas’ then there are numerous cases of immiscible gases (Scott and van Konynenburgh 1980, page 503).

$$f_{\text{int}} = \alpha(\rho_1\rho_2)^k, \quad (6.1.1)$$

with α and k constant. There is direct experimental evidence in favor of this expression, see Section V.6. The total free energy is $f_1 + f_2 + f_{\text{int}}$. For f_1 and f_2 we shall use, in a first instance, the expressions that pertain to the respective one-component ideal gases. Thus, at equilibrium, the Hamiltonian density is

$$\rho_1 \vec{v}_1^2/2 + \rho_2 \vec{v}_2^2/2 + f, \quad f = f_1 + f_2 + \alpha(\rho_1\rho_2)^k, \quad s = \sum \rho_i S_i, \quad (6.1.2)$$

where, for the time being, the individual energy densities are those of ideal gases,

$$f_1 = \mathcal{R}_1 T \rho_1 \ln \frac{\rho_1}{T^{n_1}}, \quad f_2 = \mathcal{R}_2 T \rho_2 \ln \frac{\rho_2}{T^{n_2}}. \quad (6.1.3)$$

A great deal of attention is paid to the “**excess free energy (density)**” of a real mixture. It is defined as $f_{\text{excess}} = f - f_1 - f_2$, where f_1 and f_2 refer to situations where the individual fluids are alone with the same density and temperature. Compare Rowlinson (1959). The densities f_1 and f_2 are known in the case of ideal gases, and more or less known in other cases; yet the idea of modelling the excess, as a correction to the sum $f_1 + f_2$ is not popular. See however Lemmon (1996), Lemmon and Jacobsen (1998, 1999). For an accumulation of free energy data see Hicks and Young (1975).²

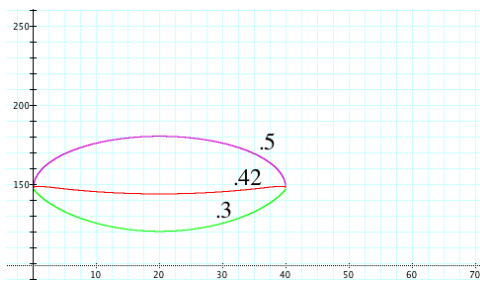


Fig.6.1.1. Free energy. The function f with $\alpha = .5, .42, .3$, $k = .56$ and fixed total density, as a function of the concentration of the mixture. The middle curve has the characteristic shape with two extrema. However, they are maxima, not minima, for either sign of α . Ideal gases are perfectly miscible and this type of interaction does nothing to alter that property.

²Unfortunately, their definition of free energy excess includes the “free energy of mixing” so that a detailed confrontation could not be made.

Following van der Waals, an alternative procedure has been to model the mixture as a single component fluid with properties that are a compromise between those of the components, with an explicit dependence of the van der Waals parameters on the molar fractions.³ This is true, in particular, of an influential paper by Scott and Van Konynenburg(1968). Note especially an expression for the excess free energy, valid in the limit of infinite pressure (Scott and Van Konynenburg 1960, p. 499), that agrees with Eq.(6.1.1), with $k = 1$.⁴

Our point of view is that a mixture, having more degrees of freedom than the one component fluid, must exhibit features that cannot be simulated by a single component, either physically or mathematically. A single-component model uses an incomplete set of dynamical variables and therefore cannot obey the fundamental relations of thermodynamics.

Lemmon *et al* (2000) include a factor T in their expression for the excess free energy, to make it look like a contribution to the entropy. A contribution to the free energy that is linear in T can always be compensated by a shift in the entropy. We shall make it a working assumption that the interaction strength is independent of the temperature.

Unfortunately, some of the concepts that help us understand non-interacting gases do not apply when interactions are present. The total pressure is well defined; it coincides with the on shell value of the Lagrangian density,

$$p = \sum \rho_i \frac{\partial f}{\partial \rho_i} - f \quad (= \mathcal{L} \text{ on - shell}). \quad (6.1.4)$$

In the present case,

$$p = \sum \mathcal{R}_i \rho_i T + (2k - 1)\alpha(\rho_1 \rho_2)^k. \quad (6.1.5)$$

This is illustrated in Fig.6.1.2 for the case that $(2k - 1)\alpha > 0$. The dependence of p on the concentration (at constant temperature and volume)

³Rowlinson voices some degree of skepticism: “Such attempts rest on the fallacy that the forces $(\alpha - \beta)$ between two molecules of species α and β are always determinable from the strengths of the forces $(\alpha - \alpha)$ and $(\beta - \beta)$.” Rowlinson does not offer an alternative but see the quoted papers by Lemmon and Jacobsen.

⁴One aspect of this approach is particularly reasonable; it is assumed that the “displaced volume” of gas number 1, represented by the coefficient b in the expression for the pressure, must be affected by the presence of gas number 2, and vice versa. I have not tried to include this effect in the calculations.

is linear in the absence of interaction; it dips below the straight line when $(2k - 1)\alpha$ is negative and it rises above it if it is positive.

But there is no natural definition of **partial pressures** and Dalton's law cannot be applied; that is one reason why the Gibbs-Dalton hypothesis is preferable; it can be formulated and suitably modified to take the interaction into account, as we have seen in Chapter V. The equations of motion, from variation of the densities, gives (6.1.2), or

$$\dot{\Phi}_i = \frac{\partial(f + sT)}{\partial\rho_i} \Big|_T.$$

In the case of a simple system we can work with the pressure or with the chemical potential as we like, but in the case of mixtures we had better get used to using the latter. In general, the pressure is one of the potentials (potential densities), not a variable.

At constant pressure, the volume as a function of concentration is often less than the sum of the volumes of the separate components. Observation of excess free energy and the deficit of volume are ready sources of information about the parameters α and k .

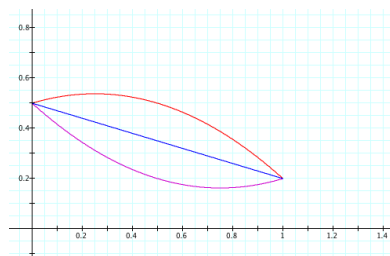


Fig.6.1.2. Pressure at constant temperature, showing the effect of interaction on the pressure profile. The abscissa is the concentration. When α is positive the upper curve illustrates the case that the exponent k is larger than .5, the lower curve the case that $k < .5$.

We shall consider the possible existence and stability of a two-phase equilibrium. After completing this simplest instance of interacting fluids with a brief Summary we shall have enough confidence to attack van der Waals' fluids in the next section.

Data

There exist collections of experimental data that can be related to the interaction density in mixtures. Before we can use it we must be sure to know what it is that is measured. A large compilation of measured values of excess energies qualifies them as values of the enthalpy (density). This choice is based on the idea that the experiments were done under circumstances where the system was in diathermic contact with the surroundings and under constant (atmospheric) pressure. That the pressure rather than the volume was fixed is easy to understand, for pressures equalizes almost instantaneously. Whether there was enough time for changes in the temperature to adjust may seem doubtful, although, if that was the express intention of the experimenters, then there is no reason why it should not be. But the action principle that has been developed, so far, is adiabatic, and we shall continue to apply it to isolated systems exclusively. The fluctuations of shortest time parameter are the adiabatic changes and they are the variations that determine the instantaneous equilibrium configuration. The postulate of minimum energy therefore refers to either the Helmholtz free energy $\int f$ (if the volume is fixed) or the Gibbs free energy $\int f + p$ (if the pressure is fixed). For simplicity we shall deal with the former case only.

The difficulty with direct experimental sources is the telegraphic nature of information. For example “The critical temperatures were observed by allowing the tubes to warm slowly in an environment of measured uniform temperature.” Neither “uniform temperature” nor “observed” are defined. Comments provided by the compiler is sometimes useful.

Conditions for equilibrium

According to the action principle a static configuration is characterized by the condition that the action must be stationary with respect to variations of the temperature and the densities. Local variations of the temperature gives the adiabatic condition. The principal statement that comes from variation of the densities is that the fields must be piecewise uniform. If the fluid separates into two parts with different concentrations then additional, global variations that remain to be investigated are variations that hold the total masses fixed, piecewise uniform variations that satisfy

$$\delta\rho_1^u = -\delta\rho_1^v, \quad \delta\rho_2^u = -\delta\rho_2^v,$$

where the superscripts u, v refer to the two parts of the fluid. This implies continuity of the pressure and the temperature and (the Euler-Lagrange

equations)

$$\text{Disc}(\dot{\Phi}_i + TS_i) = \text{Disc } \mu_i := \mu_i^u - \mu_i^v, \quad i = 1, 2.$$

The principle of maximum entropy (= minimum free energy) makes both sides equal to zero.

That both chemical momenta are continuous is the condition that a particle, of either type, at the dividing surface is subject to the same mechanical force whether it is considered to belong to one side of the boundary or the other; the continuity of $\dot{\Phi}_i - S_i T$ means that **entropic forces** are balanced as well.

To sum up, equilibrium of the divided fluid implies continuity of temperature, pressure and $\dot{\Phi}_i + TS_i - \mu_i$, $i = 1, 2$. Minimum energy implies that $\dot{\Phi}_i + TS_i$ and μ_i are separately continuous.

To solve these equations several methods can be used.

The method of the **common tangent**

The conditions of equilibrium are

$$T^u = T^v, \quad p^u = p^v, \quad \mu_i^u = \mu_i^v, \quad i = 1, 2. \quad (6.1.6)$$

We shall regard the densities as coordinates in a 2-dimensional Euclidean space and use a geometric notation. The equations of equilibrium tell us that the tangent planes to the equipotential surface $f = \text{constant}$, at the two points, are parallel (See Section IV.4.) Now

$$p = (\mathcal{R}_1 \rho_1 + \mathcal{R}_2 \rho_2) T + \alpha (2k - 1) (\rho_1 \rho_2)^k, \quad (6.1.7)$$

Since $p = \rho_1 (\partial f / \partial \rho_1) + \rho_2 (\partial f / \partial \rho_2) - f$ it follows that

$$f(\rho_1, \rho_2)^u - f(\rho_1, \rho_2)^v = (\rho_1^u - \rho_1^v) \mu_1^v + (\rho_2^u - \rho_2^v) \mu_2^v.$$

That is, the two tangent planes actually coincide. This is exactly the same situation that occurs in saturation, as illustrated in Fig.4.3.1 and subsequent figures, but in a higher dimension, making illustration more difficult.

As an example we may take $\beta = 2$, $k = 1$ and thus $\alpha = 2\mathcal{R}T/\rho$. The concentrations at the minima of f in Fig.6.1.3 are $x = .24853$ and $y = .75147$. The pressure is $\mathcal{R}\rho T + \alpha\rho_1\rho_2 = \mathcal{R}$, so that the excess pressure at fixed volume must be more than twice the pressure of the corresponding ideal,

non interacting mixture. It is likely that, when this condition is met, one or both of the real gases will be in the domain where they must be described by the van der Waals equation of state.

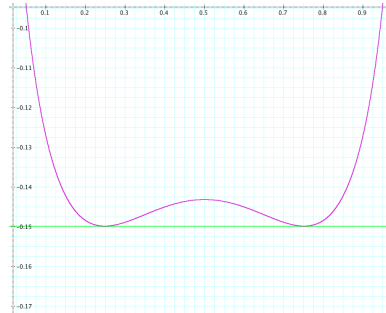


Fig.6.1.3. **Common tangent.** Example, $\beta = 2, k = 1$; the dependence of f on the concentration, on the line $\rho_1 + \rho_2 = 1$. The free energy density has been normalized to give the tangent zero slope.

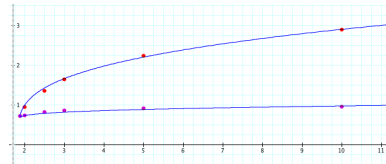


Fig.6.1.4. The range of values of the parameters k (abscissa) and β (ordinate) for which the free energy density exhibits two minima is the interval between the two lines.

For assigned values of the parameters α, k there is a finite range of values of β ; if $k = 1$ it is, approximately,

$$2 < \frac{\alpha}{\mathcal{R}T} \rho^{2k-1} < 10.$$

This is the range of temperatures for which separation occurs. The upper limit is referred to as UCST or upper critical solution temperature. At this temperature any decrease in the temperature converts the system from a homogeneous liquid to a two phase system. The lower limit, L(ower)CST the same transformation takes place when the temperature is increased. (Scott and Van Konynenburg 1968)

Symmetry

It happens that the formula for the pressure, when expressed in terms of molar densities, is symmetric with respect to the interchange of the two densities; the fact that $p^u = p^v$ strongly suggests that we look for solutions that satisfy

$$(\rho_1^u, \rho_2^u) = (\rho_2^v, \rho_1^v). \quad (6.1.8)$$

For a determination of equilibrium using (6.1.8) see Fig.6.1.5. This method is seldom applicable.

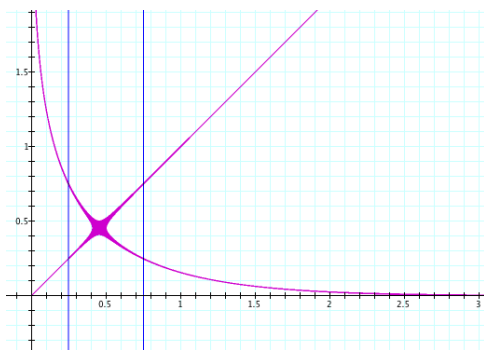


Fig. 6.1.5. Determination of concentrations using symmetry. The curve is the locus of pairs of densities that satisfy the symmetry condition Eq.(6.1.8). The two vertical blue lines mark the values of x with the selected value of the pressure. The coexistent densities are the coordinates of the intersections.

Direct search

Both methods used so far to find the coexistent mixtures depend on symmetry, on the assumption that the two coexistent mixtures have conjugate concentrations, $(\rho_1, \rho_2)^u = (\rho_2, \rho_1)^v$. But there are other solutions, and to find them all we know of no method better than the following. We produce plots of the loci defined by the three equations

$$\mu_1(x, y) = A, \quad \mu_2(x, y) = B, \quad p(x, y) = C,$$

where A, B, C stand for real numbers. These numbers are adjusted so that the first two curves intersect at 2 points; then they are adjusted further until an isobar passes through both of them. For an illustration, see Fig.6.1.6.

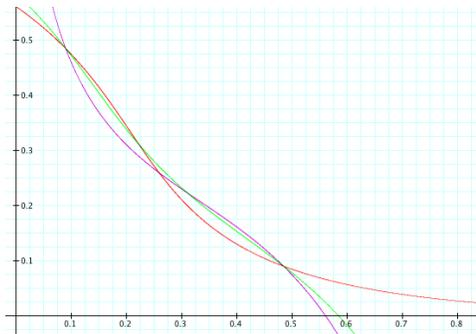


Fig 6.1.6. A typical determination of **co-existence**. The ordinates are the two densities. The red lines are loci of the chemical potentials, the green line is an isobar. The two triple intersections are the densities of two coexistent densities. The geometry is typical of immiscibility, as opposed to condensation of one of the constituents.

This method is the more rewarding, for it will give us a visual representation of the nature of the physical phenomenon. We shall refine this scheme and carry out the calculations in several particular cases later.

Summary.

We have explored a simple phenomenon that involves a mixture of two ideal gases, slightly modified by a simple interaction term added to the free energy. In this case we have verified, under certain circumstances, the separation of the mixture into two parts with quite different concentrations. What makes real gases more complicated, and more interesting, is the fact that interactions between like particles also come into play, in a regime not too far from saturation, where the individual fluid components behave, approximately, like van der Waals fluids. In fact, it is commonly believed that the phenomenon of immiscibility cannot occur in fluids above the condensation point. It is even said that it does not happen with gases; what lies behind this is a too restricted definition of “gas”.

What about the entropies of these mixtures? It would be naive to suppose that the Gibbs-Dalton law applies, since we expect that it is affected by the interaction. Fortunately, as was we have seen, and as we shall confirm below, it is not necessary to know the entropies in the present investigation. What we need to know about the entropy was discussed above; it led to the statement that the chemical potentials are continuous.

VI.2. Mixture of two van der Waals fluids.

The spinodal of unaries

Refer to Fig. 6.2.1; it is the same as Fig.4.3.1, with additions. The curve is the van der Waals potential, the function $p(\rho, T)$ for a fixed value of T . This function is some times referred to as an equation of state, which is misleading since ρ, T is not the natural set of variables for the pressure - the natural variables are μ and T .

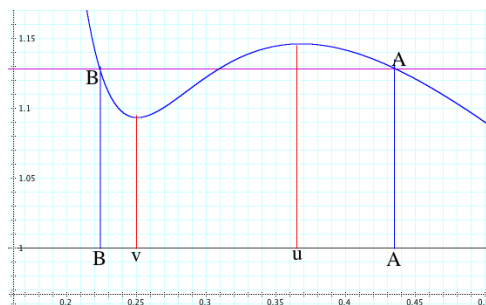


Fig.6.2.1. From Chapter 4; with the points of the spinodal added; it is the manifold that consists of the two points u and v on the density axis defined by (6.2.1). The abscissa is the inverse density. The temperature is fixed below critical.

The points A and B in the figure are the points of coexistence for the chosen temperature; both p and μ have the same values at both points. They define a pair of stable configurations in equilibrium with each other. A very useful concept is the “**spinodal**”; in the present case it is the set of densities labelled u, v , points at which $\partial p / \partial \rho|_T = 0$. A better characterization of this manifold is,

$$\frac{\partial^2 f}{\partial \rho^2} \Big|_T = 0 \quad (6.2.1)$$

(note that $\partial p / \partial \rho|_T = \rho \partial^2 f / \partial \rho^2$); it has the advantage of being defined by the free energy as a function of its natural variables and it has a simple and natural generalization to mixtures.

The most important property of the spinodal is the following. The two points are bracketed by the points A, B ; the unstable point between A and B lies between the spinodal points and this gives a fairly accurate indication of the location of the points of coexistence once the spinodal is known. As

the temperature is raised, points A and B approach each other and coalesce with the spinodal (points u and v) at T_{cr} .

The mapping $p \rightarrow \rho$ is 3-valued when the pressure is between the values $p(u)$ and $p(v)$, one-valued when the density is outside this interval

The spinodal of binaries

The set of 2-phase configurations of a typical binary system, for each pair of values p, T , is a one-dimensional subset of the density plane. Since, in the case of van der Waals fluids, $x = b_1\rho_1$ and $y = b_2\rho_2$ take values between 0 and 1, we shall use coordinates x, y with this range, $0 < x, y < 1$ and refer to $\vec{\rho} = (x, y)$ as a point in density space.

For fixed T below a certain limit T_{max} , the density space of a typical binary system is divided into 3 or more distinct regions, separated and sometimes bounded by points of the spinodal, this being the locus of points on which

$$\det \left(\frac{\partial f}{\partial \rho_i \partial \rho_j} \right)_T = 0,$$

the natural generalization of (6.2.1). These are points where the mapping $\vec{\mu} \rightarrow \vec{\rho}$ is 2-valued. They form lines that separate a single valued domain from a 3-valued domain. The spinodal is not the line of coexistence, but it gives a good indication of where the coexistent mixtures are, and it has the advantage of being easy to calculate and to plot.

Here is an example of what is observed in a typical experiment. The experimenter usually begins with a homogeneous mixture at low pressure, a gaseous system with fixed concentration. Because the concentration cannot be easily manipulated it is natural to use the concentration as one of the variables, another being the total density or its inverse, the volume. The temperature may be kept fixed while the pressure is slowly increased to take the system through a sequence of adiabatic equilibria.

As the pressure is increased (with T fixed) the system typically traces a radial line in **density space**. Eventually, as the density approaches the spinodal, condensation sets in; this point is referred to as **the dew point**. At best, the droplets fall like rain and accumulate at the bottom of the vessel.

The next three diagrams show what happens to a model of an Ethane-Propane mixture in the 2-dimensional density space. The oval (purple) is the spinodal of the mixture. As the temperature is raised the oval contracts and reduces to a point at a temperature $T_{max} = 370.5$, above which no phase separation occurs. When T is reduced to 369.5, which is the critical temperature of Propane, the oval touches the vertical axes; at lower temperatures the oval is a horizontal band across density space.

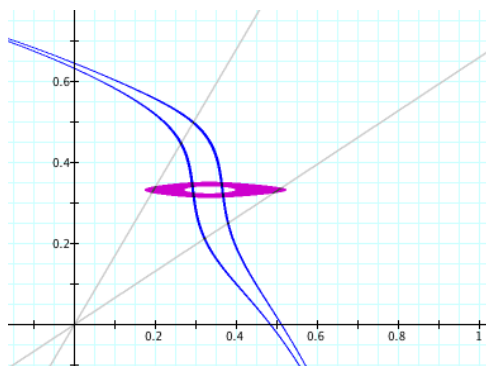


Fig. 6.2.2. Density diagram for the model of the mixture of methane (abscissa) and propane (ordinate) at $T = 370.4, \alpha = 5$, showing the spinodal (purple) and two (blue) isobars. The other curves are loci of one of the two chemical potentials. The spinodal is a closed line bordering an oval. Radials indicate critical concentrations for this value of T .

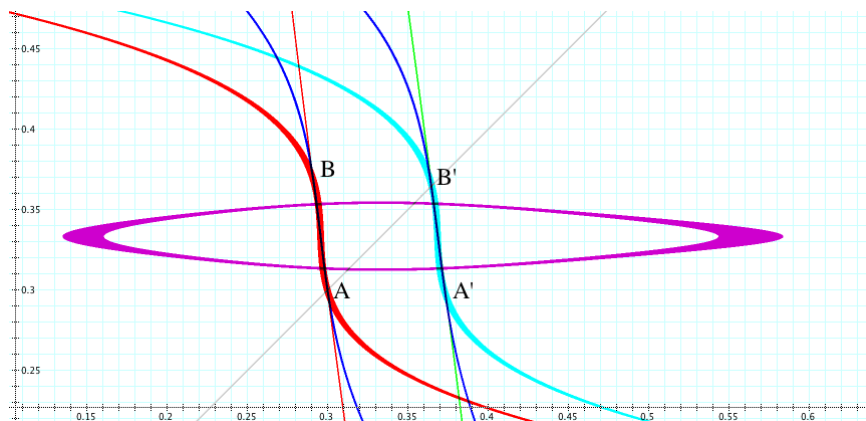


Fig.6.2.3. Density diagram for (the same model of) the mixture of methane and propane at $T = 370, \alpha = 5$. If the temperature is lowered to 369.5, which is the **critical temperature** of propane, then the spinodal reaches the vertical axis and below that temperature it is a nearly horizontal band that reaches

across the entire interval $0 < x < 1$. The blue lines are isobars, the red ones and the light blue ones are loci of the chemical potentials.

The slope of the radial line in Fig. 6.2.3 is the concentration ρ_2/ρ_1 . In the most standard type of experiment the system moves out along a radial line as the pressure is increased. If the radial line intersects the spinodal oval, then the system moves along the radial until, before quite touching the spinodal, it reaches a point of condensation, the dew point, shown in Fig. 6.2.3 as A , with density $\bar{\rho}^u = (x^u, y^u)$.

What happens next, as the pressure is further increased, is this. In addition to the gas at the point $A = \bar{\rho}^u$ there appears a liquid at the point $B = \bar{\rho}^v$, on the same isobar. Initially the population of this point; that is, the total amount of liquid with this density, is negligible, but with increasing pressure the system gradually transfers, by condensation, from A to B . To maintain the average concentration of the total sample this transfer is accompanied by a movement of both points towards the right, along “lines of coexistence” at a nearly constant distance from the spinodal. This continues until the upper point reaches the radial of the original concentration (the continuation of the original radial line) at which point the condensation is complete and the whole system is at the point B' , the bubble point. The lower point of coexistence has moved from the original point A to reach the point A' (on the same isobar as B') with the occupation diminishing to zero. Further increasing the pressure does not lead to any unusual phenomena, the liquid remains homogeneous, moving along the original radial line, upwards from B' .

At lower temperatures the spinodal reaches the vertical axis, at $T = 369.5$, the critical temperature of Propane, as well as the vertical line $x = 1$. At still lower temperatures it approaches the horizontal axis at $T = 306$, the critical temperature of Ethane, as shown in Fig.6.2.4

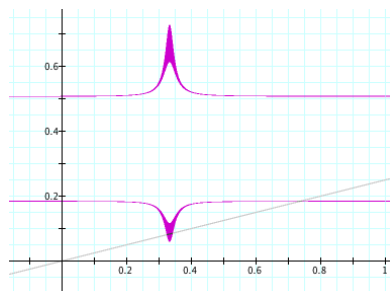


Fig.6.2.4. As the two preceding figures but the temperature is slightly above the critical temperature of Ethane.

Experimental reports often give much less information, most experiments are stopped on reaching the dew point, to record the dew point pressure at the chosen temperature. In a companion experiment one starts with a homogeneous liquid at high pressure and traces out the approach to the point B' , **the bubble point**. The actual separation is often not observed. Results are presented as a T, p graph.

Calculation of the line of coexistence

The theoretical calculation of the points of **coexistence** is painful without the assistance of an appropriate computer. These points are defined by the conditions of equilibrium,

$$T^u = T^v, \quad p^u = p^v, \quad \bar{\mu}^u = \bar{\mu}^v.$$

The best strategy that was found is the following. Choose a value of T and an isobar and select a point $\vec{\rho}_0$ on it. Experience allows to select a point fairly close to the line of coexistence. Draw the loci (all for fixed T and $\vec{\rho}_0$)

$$p(\vec{\rho}) = p(\vec{\rho}_0), \quad \mu_1(\vec{\rho}_1) = \mu_1(\vec{\rho}_0), \quad \mu_2(\vec{\rho}) = \mu_2(\vec{\rho}_0).$$

The last two should have two further intersections, one inside the spinodal (ignore it) and one on the upper side. This latter will probably not lie on the same isobar; in that case slide to point $\vec{\rho}_0$ along the chosen isobar until the required triple intersection is achieved on the upper side. This locates a pair of co-existent concentrations, the points A and B . The points A' and B' are easily determined since they are known to be on the radial line of the original, average concentration.

VI.3. Sample applications - first example

This is all about mixtures of van der Waals fluids. The experimental literature is vast, but much of it reports only partial results; there is very little observation of actual separation. Theoretical attempts are, for the most part, applications of van der Waals' one - fluid method that we have already mentioned; more shall be said about this below. There have been many attempts to account for the data using variations of the van der Waals

approach. Because these theories are phenomenological, and consequently subject to few constraints, they are often successful in reproducing selected data. The attempts reported here are also less than completely successful but the work is far from complete.

In this Section we continue to base the approach on the action principle, with a complete set of thermodynamical variables, with the approach to mixtures of Chapter V and with the component unaries modeled as van der Waals fluids. Because we aim at making predictions, we must restrict the number of free parameters; consequently our first attempt uses the following expression for the free energy density,

$$f = f_1 + f_2 + f_{int}, \quad f_{int} = \alpha \rho_1 \rho_2.$$

There is only one free parameter, α , the van der Waals parameters in f_1 and in f_2 are determined by observations of the pure components. The interaction term is of the type used by others, but much more restricted; compare Scott and van Konigenburg's

$$f_{int} = Q(c)\rho^2,$$

where ρ is the total density, c is the concentration and Q is a polynomial – and these are not the only adjustable parameters.

Here we shall examine some mixtures of the simplest **organic fluids**.

Table 1: Critical parameters

Methane	16	190.6	4.63	7.83	.229	.0427
Ethane	30	306	4.96	5.21	.550	.0640
Propane	44	369.5	4.52	3.95	.877	.0844
Butane	58	25.1	3.58	2.72	1.466	.123

Table 1. Units are MPa for pressure, MPa(Lit/mol)² for a and (mol/Lit) for b . The figures are consistent with van der Waals' formula within 1 percent.

The **vapor pressures** of ethane and propane are calculated from the van der Waals formula and collected in the following Table.

Table 2: Vapor pressure

Ethane	T	306	290	270	250	220	200
p		4.97	4.00	2.96	2.12	1.14	.7
Exp.		4.96	3.51	2.20	1.30	.49	.22
Propane	T	369.5	360	340	320	300	280
p		4.55	4.1	3.23	2.49	1.87	1.35
Exp.		4.09	3.5	2.42	1.58	.98	.624

Table 2. Vapor pressure of Ethane and Propane. “Exp.” stands for experimental results. As an approximation to the real, unary fluids, the van der Waals model is successful in the qualitative sense. Quantitatively, it usually reproduces the experimental properties to better than 10 percent accuracy near the critical temperatures, better at higher temperatures but progressively less well at lower temperatures. Our hope is to develop a model of the mixtures with a comparable degree of agreement with experiments.

‘Experimental value of the pressure’. For propane, these are very difficult to find; and most of the discrepancy arises from the inconsistency of the few experimental figures. For consistency the numbers 4.55 and 4.09 in the first column should have been equal. Pressure in MPa. As an approximation to the real, unary fluids, the van der Waals model is successful in the qualitative sense. Quantitatively, it usually reproduces the experimental properties to better than 10 percent accuracy near the critical temperatures, better at higher temperatures but progressively less well at lower temperatures. Our hope is to develop a model of the mixtures with a comparable degree of agreement with experiments.

Binary van der Waals mixtures. Formulas

For a mixture of any two van der Waals fluids, the assumed free energy density is

$$f = f_1 + f_2 + \alpha \mathcal{R}(\rho_1 \rho_2)^k, \quad (6.3.1)$$

$$f_1 = \mathcal{R}T \rho_1 \ln \frac{\rho_1}{(1 - b_1 \rho_1) T^{n_1}} - a_1 \rho_1^2, \quad f_2 = \mathcal{R}T \rho_2 \ln \frac{\rho_2}{(1 - b_2 \rho_2) T^{n_2}} - a_2 \rho_2^2, \quad (6.3.2)$$

with the constant α of order unity and $k = 1$. To simplify we set $x = b_1 \rho_1$, $y = b_2 \rho_2$. We also drop the factor T^n in the logarithm since it makes

no contribution to the determination of the equilibrium,

$$f_1 = \frac{\mathcal{R}}{b_1} \left(Tx \ln \frac{x}{1-x} - \frac{27}{8} T_1 x^2 \right), \quad f_2 = \frac{\mathcal{R}}{b_2} \left(Tx \ln \frac{y}{1-y} - \frac{27}{8} T_2 y^2 \right)$$

and

$$f = \frac{\mathcal{R}}{b_1} \left(Tx \ln \frac{x}{1-x} - \frac{27}{8} T_1 x^2 \right) + \frac{\mathcal{R}}{b_2} \left(Tx \ln \frac{y}{1-y} - \frac{27}{8} T_2 y^2 \right) + \alpha \mathcal{R} \left(\frac{xy}{b_1 b_2} \right)^k;$$

T_1 and T_2 are the critical temperatures of the constituents. The derivatives of the free energy density are, when the exponent k in (6.2.1) is unity,

$$\mu_i(x, y) = \mathcal{R}T \left(\ln \frac{\rho_i}{(1 - b_i \rho_i) T^{n_i}} + \frac{1}{1 - b_i \rho_i} \right) - 2a_i \rho_i + \alpha \mathcal{R} \rho_j, \quad i, j = 1, 2 \text{ or } 2, 1.$$

and

$$f_{ii} = \frac{\mathcal{R}T}{\rho_i (1 - b_i \rho_i)^2} - 2a_i, \quad i = 1, 2, \quad f_{12} = \alpha \mathcal{R}.$$

The thermodynamic pressure is

$$\frac{p}{\mathcal{R}} = \frac{1}{b_1} \left(T \frac{x}{1-x} - \frac{27}{8} T_1 x^2 \right) + \frac{1}{b_2} \left(T \frac{y}{1-x} - \frac{27}{8} T_2 y^2 \right) + \frac{\alpha}{b_1 b_2} xy.$$

The spinodal, a two-dimensional manifold in the 3-space with coordinates T and the two densities, is defined by

$$\det \left(\frac{\partial^2 f}{\partial \rho_i \partial \rho_j} \right) = 0.$$

In a form suitable for the computer,

$$f_{11} = \mathcal{R}b_1 \left(T \frac{1}{x(1-x)^2} - \frac{27}{4} T_1 \right),$$

$$f_{22} = \mathcal{R}b_2 \left(T \frac{1}{y(1-y)^2} - \frac{27}{4} T_2 \right).$$

and $f_{12} = f_{21} = \alpha$. The spinodal is thus the locus

$$b_1 b_2 \left(\frac{T}{x(1-x)^2} - \frac{27}{4} T_1 \right) \left(\frac{T}{y(1-y)^2} - \frac{27}{4} T_2 \right) = \alpha^2. \quad (6.3.3)$$

For a fixed value of T it is empty unless T is less than a ‘‘maximal’’ value that, for the Ethane/Propane mixture with $\alpha = 10$, is

$$T_{max} = 375.4K$$

Table 3: Maximal temperature

α	1	2	5	10	50
T_{max}	369.6	369.8	371.1	375.4	443.6
p/\mathcal{R}	1661	1685.5	1765	1930	2860
p	13.81	14.01	14.67	16.05	23.78

The variation of this with the strength of the interaction is shown in the Table.

Table 3. **Maximal temperature**, being the highest temperature at which separation occurs, for Ethane/Propane with varying interaction strength.

At this value of T the spinodal is a single point at $x = y = 1/3$. Below this value the single point opens to a closed oval, as shown in Fig.6.2.2-3. Both figures also show two isobars, each of which cuts the oval. Straight lines from the origin are lines of constant concentration; in Fig.6.2.2 they are tangent to the ovals.

Coexistence

The conditions for coexistence of two mixtures is the continuity of T, p and

$$\mu_i(x, y) = \mathcal{R}T \left(\ln \frac{\rho_i}{(1 - b_i \rho_i) T^{n_i}} + \frac{1}{1 - b_i \rho_i} \right) - 2a_i \rho_i + \alpha \rho_j, \quad i, j = 1, 2 \text{ or } 2, 1.$$

An efficient way to perform the calculation was already presented.

The dynamical variables have the following values at points A, A', B, B' , in Fig.6.2.3.

Table 4: Maximal temperature

<i>Point</i>	x^u	y^u	p/R
A	.37	.3	1658
B	.291	.370	
A'	.373	.294	1847
B'	.364	.364	

Table 4. The two pairs of coexistent mixtures for given initial low density, 50-50, gaseous, model mixture of ethane and propane. Most experiments measure only the pressure.

Points that are **critical** to the experimenter

In a region of temperatures just below T_{max} the spinodal is an oval, simply connected and convex. In a typical experiment one starts with a low pressure and low densities, x and y normalized molar densities less than 1/3. The mixture is homogeneous. The pressure is increased, or the temperature is increased, or both, but the concentration is kept fixed. One is moving out from the origin of the density diagram along one of the radials. This radial may cross the spinodal or it may pass to the left or to the right of it. In the first case separation will occur at a point below the spinodal; what happens here was described in Section VI.2. Figs 6.2.2 and 6.2.3 illustrate this in the case of a model.

As the temperature is changed the intersection of any radial line eventually becomes tangent to the spinodal. The meniscus disappears if this point is very close to the spinodal, as in Fig.6.2.2; at that point the densities of liquid and gas become equal; these are the critical points reported by the experimenter. As the temperature descends to T_2 , the critical temperature of the least volatile gas, the oval reaches the vertical axis. Below this temperature there is an interval of temperatures where the oval still may have a radial tangent at the high end, at very high pressures, then this also disappears. At still lower temperatures, as we approach the critical point of the other gas, it returns. See Fig.6.2.4.

This behavior of the model is in contradiction with experiments. We must conclude that our first choice of f_{int} is inappropriate, but before looking for alternatives we shall look briefly at another example, the Argon-Oxygen system.

The critical points to the experimenter are the configurations at which the radials determined by the concentration are tangent to the spinodal oval. They are uniquely determined by the temperature, at least for temperatures close to T_{max} . Figs 6.2.2-4 show the shape of the spinodal for a descending series of temperatures, for a model that has $f_{int} \propto \rho_1 \rho_2$.

Remark. The study of mixtures in terms of expressions for the free energy are legion in the literature. It is unexpected, however, to encounter an approach that is phenomenological to the point that additional input, an

“equation of state” or more precisely an expression for the pressure, is needed (Hicks and Young 19); this even in the case that the inspiration comes from van der Waals and the free energy had already been used. In thermodynamics, the pressure is determined by the free energy density, $p = \vec{\rho} \cdot \vec{\nabla} f - f$. But the ‘free energy’ of the one-fluid model is not the thermodynamic free energy and the one field model is not thermodynamics. Consequently, the formula that is used to calculate the critical points is without justification. Separate phenomenological input (with additional adjustable parameters) is invoked in the form of an independent relation between pressure and temperature.

VI.4. Second mixture of van der Waals fluids

The plan for this section is not just to study another mixture, but to consider another type of interaction.

Here we examine mixtures of Argon and Oxygen. These two gases have approximately the same van der Waals parameters.

Gas number 1, Argon, $\mu_1 = 40$, $n_1 = 3/2$, $T_1 = 150K$, $p_1 = 4.9MPa$, $a_1 = 1.355$, $b_1 = .03201$. and

Gas number 2, Oxygen, $\mu_2 = 32$, $n_2 = 5/2$, $T_2 = 155K$, $p_2 = 5MPa$, $a_2 = 1.382$, $b_2 = .03186$.

The units are *bar.liter*²/*mol*² for *a* and liter/*mol* for *b*.

We begin by examining the spinodal isobars, Eq. 6.4.1:

$$b_1 b_2 \left(\frac{T}{x(1-x)^2} - \frac{27}{4} T_1 \right) \left(\frac{T}{y(1-y)^2} - \frac{27}{4} T_2 \right) = \alpha^2. \quad (6.4.1).$$

this relates α directly related to T_{max} , the highest temperature at which separation can occur at any concentration, the critical temperature We should like to begin by choosing the best value of the coupling strength α . Unfortunately, this is rarely measured. Jones and Rawlinson (196) tell us only that T_{max} is higher than 149.4K; our model says that it is higher than 155. the Table relates T_{max} to α .

Table 5. The highest temperature at which separation occurs, as a function of the strength of the interaction $f_{int} = \alpha \rho_1 \rho_2$.

Fig 6.4.1 shows the spinodal for $\alpha = .016$, $T = 160K$. In Fig.6.4.2 $T = 155K$, which is the critical temperature of Oxygen, the spinodal oval

Table 5: Effect of strength of interaction

T_{max}	α
155.2	.001
156.0	.0032
160.0	.0098
164.2	.0160
171.2	.0260
179.6	.0380
186.7	.048

has grown to reach the vertical axis. In Fig. 6.4.3 the temperature is 149.4K, the highest temperature recorded by Jones and Rawlinson. The blue line is the locus of the concentration, value .202 as in the experiment. According to observation, this is a critical point so we expect it to be nearly tangent to the spinodal. Since the temperature is below the critical temperature (155K) of oxygen, this is in clear disagreement with the model.

Fig.6.4.1. The spinodal for a temperature slight lower than critical.

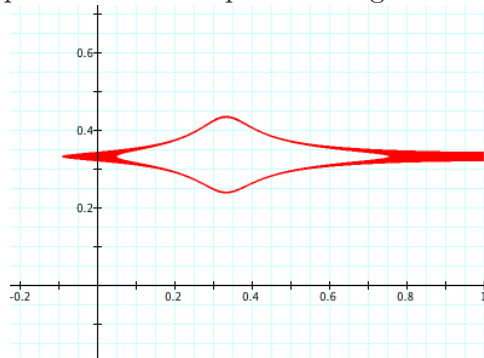


Fig.6.4.2. As preceding Figure but $T = T_2 = 155K$.

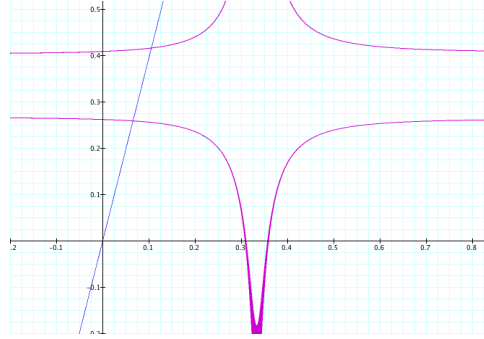


Fig. 6.4.3. Here $T = 149.4$. the radial line indicates the concentration in the experiment of Jones and Rowlinson.

Later we shall attempt to understand the propagation of sound in mixtures, with the same model and the same interaction as we have used here, $f_{int} = \alpha\rho_1\rho_2$, to find that it cannot account for sound propagation either. Instead, what works very well for the speed of sound is

$$f_{int} = \alpha\sqrt{\rho_1\rho_2}.$$

Although the success of this model in accounting for the speed of sound refers to experiments at room temperature, it is natural to ask what it can do for the critical phenomena being discussed here. Indeed, our approach obliges us to use the same Lagrangian for both phenomena. as we have stressed, this is an essential feature of our method, the main source of a greatly enhanced predictive power.

The square root interaction density for mixtures

It was natural to expect that the expression for the interaction energy take the same form as the self-interaction energy in van der Waals formula. That is why we have given this idea a fair hearing, to see it fail. We already had some experience with sound propagation that suggested a different form for f_{int} (Fronsdal 2011). To test the idea that the same Lagrangian density must serve for both phenomena we now investigate the viability of

$$f_{int} = \mathcal{R}\alpha\rho_1\rho_2 + \mathcal{R}\alpha'\sqrt{\rho_1\rho_2},$$

with α provisionally equal to zero. The chemical potentials

$$\mu_1 = f_1 = \mathcal{R}T \left(\ln \frac{\rho_1}{(1 - b_1\rho_1)T^{n_1}} + \frac{1}{1 - b_1\rho_1} \right) - 2a_1\rho_1 + \mathcal{R}\frac{\alpha'}{2}\sqrt{\rho_2/\rho_1},$$

$$\frac{f_{11}}{\mathcal{R}} = b_1 \left(\frac{T}{x(1-x)^2} - \frac{27}{4}T_1 \right) - \frac{\alpha'}{4} \sqrt{b_1^3/b_2} \sqrt{y/x^3},$$

$$\frac{f_{12}}{\mathcal{R}} = \frac{\alpha'}{4} \sqrt{b_1 b_2} / \sqrt{xy}.$$

and the spinodal is the locus

$$f_{11}f_{22} = \left(\frac{\alpha'}{4} \right)^2 \frac{b_1 b_2}{xy}$$

or

$$\left(\frac{T}{x(1-x)^2} - \frac{27}{4}T_1 - \sqrt{\frac{b_1}{b_2}} \frac{\alpha'}{4} \sqrt{\frac{y}{x^3}} \right) \left(\frac{T}{y(1-y)^2} - \frac{27}{4}T_2 - \sqrt{\frac{b_2}{b_1}} \frac{\alpha'}{4} \sqrt{\frac{x}{y^3}} \right) = \left(\frac{\alpha'}{4} \right)^2 \frac{1}{xy}.$$

To interpret it we need isobars. The pressure is independent of the interaction, simply

$$\frac{p}{\mathcal{R}} = \frac{1}{b_1} \left(\frac{x}{1-x} T - \frac{27}{8} T_1 x^2 \right) + \frac{1}{b_2} \left(\frac{y}{1-y} T - \frac{27}{8} T_2 x^2 \right).$$

The expression for the μ_i are

$$\frac{\mu_1}{\mathcal{R}T_1} = \frac{T}{5.19} \left(\ln \frac{x}{1-x} + \frac{1}{1-x} \right) - \frac{27}{4}x + 36.0321 \sqrt{\frac{20}{50}} y + .03112 \frac{\alpha'}{\mathcal{R}} \sqrt{\frac{y}{x}}$$

$$\frac{\mu_2}{\mathcal{R}T_2} = \frac{T}{290} \left(\ln \frac{y}{1-y} + \frac{1}{1-y} \right) - \frac{27}{4}y + 1.38765 \sqrt{\frac{20}{50}} x + .001334 \alpha' \mathcal{R},$$

The formulas that we need are the free energy,

$$\hat{f} = \frac{fb_1}{\mathcal{R}T_{c1}} = T_r x \ln \frac{x}{1-x} - \frac{27}{8} x^2 + b \left(T_r y \ln \frac{y}{1-y} - c \frac{27}{8} y^2 \right) + \beta xy, \quad (cf)$$

the chemical potentials,

$$\mu_x(x, y) = T_r \left(\ln \frac{x}{1-x} + \frac{1}{1-x} \right) - \frac{27}{4}x + \beta y,$$

$$\mu_y(x, y) = b T_r \left(\ln \frac{y}{1-y} + \frac{1}{1-y} \right) - bc \frac{27}{4}y + \beta x,$$

the second derivatives,

$$f_{xx} = \frac{T_r}{x(1-x)^2} - \frac{27}{4}, \quad f_{yy} = b \frac{T_r}{y(1-y)^2} - bc \frac{27}{4}, \quad f_{xy} = \beta,$$

and the pressure,

$$\frac{pb_1}{\mathcal{R}T_{c1}} = T_r \left(\frac{x}{1-x} + b \frac{y}{1-y} - \frac{27}{8} (x^2 + bcy^2) \right) + \beta xy.$$

Reasonable agreement with the observations of Jones and Rowlinson is obtained with $\alpha = 120$, as shown in the Table and in Figs 6.4.4-7.

The 4 experiments are illustrated by the plotting of the spinodal (purple) and the relevant isobar (blue) in the density plane, in Figs 6.4.4-7. Each radial (green) line is the path followed during one of the the experiments, in which the concentration is constant. The experiment started at low density and pressure and was terminated at the dew point.

Table 6: Results from the square root model

T	p	c	Exp.
132.0	520	.77	.798
138.0	760	.70	.599
143.8	865	.34	.401
149.4	1100	.19	.202

TABLE 6. The square root model with $\alpha = 120$. The third column is the (molar) concentration $c = x/x + y$. The temperatures are those of the experiment and the last column are the experimental concentrations. Experimental values of the pressure are not available.

Quantitatively, the model agrees very well with the measurements. The shape of the spinodal is quite different in this model and this is the type of structure that is needed to account for the experiment of Jones and Rowlinson. It may be noted that the geometry exhibited at the first two points is quite different from the last two points; something that cannot be revealed by the experiment.

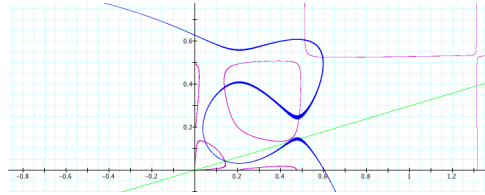


Fig. 6.4.4. Here $T = 149.4$.

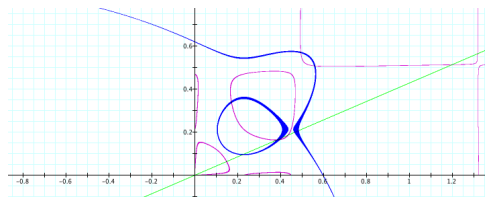


Fig. 6.4.5. Here $T = 143.8$.

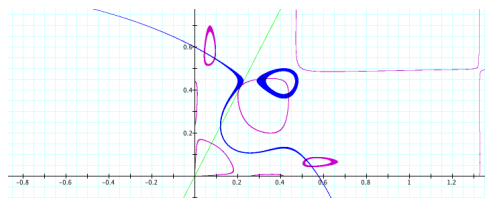


Fig. 6.4.6. Here $T = 138K$.

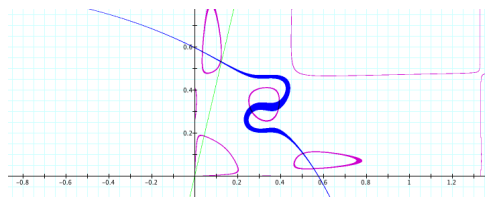


Fig. 6.4.7. Here $T = 132K$.

Nitrogen and Argon

This case is very similar but there is less experimental information available.

Gas number 1, Nitrogen, $\mu_1 = 34$, $n_1 = 5/2$, $T_1 = 126.3$, $b_1 = .03913$.
Gas number 2, Argon.

Taking $\alpha' = 100$ we get a good fit to 3 out of four experimental points.

Table 7: N and Ar, square root model

T	p	c	Exp.
131.0	580	.58	.8
134.5	600	.42	.6
141.0	865	.4	
146	1100	.30	.2

Table 7. Nitrogen and Argon. The first 3 column gives the result of our model; the last is experimental.

These bare numbers do not give an idea of the complicated picture that is illustrated in Figs 6.4.8-10. The picture changes very rapidly with the input parameters, so that experimental uncertainties play a role.

We conclude that the Lagrangian with a square root interaction is in qualitative agreement with measurements if the interaction strength α' is near $100(cm/sec)^2$. Later we shall see that the same Lagrangian can account for the speed of sound in the mixture.

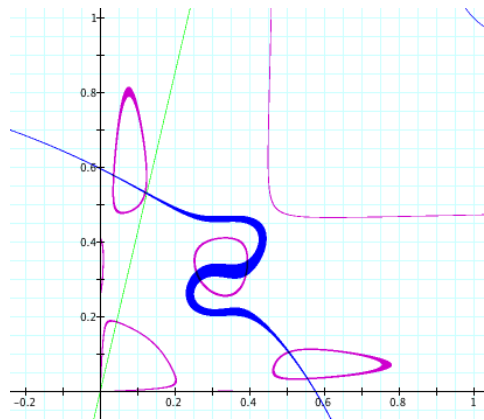


Fig.6.4.8. The singular point for $T = 146$ and $\beta = \pm 3$.

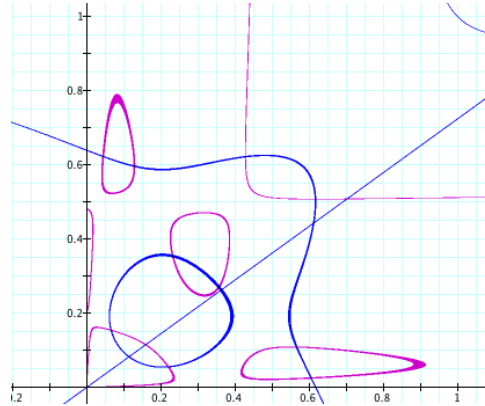


Fig.6.4.9. The singular point. for $T = 134.5$ and $\beta = \pm 3$.

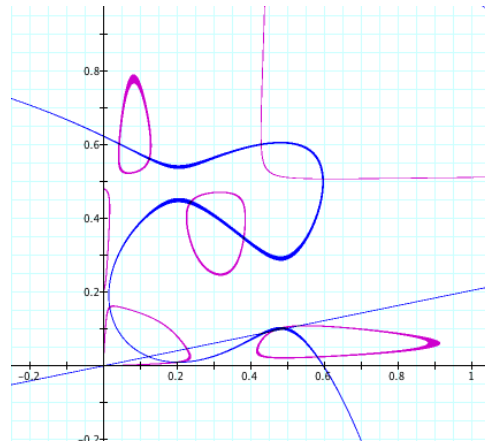


Fig.6.4.10. The singular point. for $T_r = 146$ and $\beta = \pm 3$.

Fig 6.1.6 is a clear example to show what happens near a critical point. We plot loci of μ_1 (red curves) and μ_2 (blue curves), for the same value of T , α and densities $(x, y) = (a, .6a)$. This is the value of x at the point where the line $y = .6x$ nearly touches the closed line. It is the case shown in Fig.6.1.6, where the three loci of μ_1, μ_2 and p are seen to touch, and in Fig.6.4.3. It is a critical point of the set of configurations that is projected out by fixing the relative concentration to $y/x = .6$.

This scenario is close to the experimental situation. One begins with a homogeneous mixture at the higher temperature and reduces the temperature

very slowly. At the critical temperature condensation sets in, the 10-to-6 homogeneous mixture seizes to be stable.

VI.5. Helium and Xenon

Critical parameters:

$$\begin{aligned} \text{He: } T_{cr} &=: T_1 = 5.19K, & p_{cr} &= 2.24atm = 227kPa, \\ \text{Xe: } T_{cr} &=: T_2 = 289.8K = 16.6C, & p_{cr} &= 57.6atm = 5840kPa. \end{aligned}$$

Van der Waals parameters:

$$\text{He: } a_1 = .0346barLit^2/mol^2, \quad b_1 = .0237Lit/mol$$

,

$$\text{Xe: } a_2 = 4.250barLit^2/mol^2, \quad b_2 = .05105Lit/mol$$

.

$$\textbf{Interaction } f_{int} = \mathcal{R}\alpha\rho_1\rho_2$$

This is a mixture that has been difficult to deal with; the van der Waals approach has not been successful. We begin by briefly confirming this within our framework.

The free energy density is thus $f = f_1 + f_2 + \mathcal{R}\alpha\rho_1\rho_2$.

The maximal (critical) temperature

The maximal temperature of the mixture is the lowest temperature for which the determinant of the matrix of second partial derivatives of the free energy is positive definite, at this point

$$b_1 b_2 \left(\frac{T}{x(1-x)^2} - \frac{27}{4} T_1 \right) \left(\frac{T}{y(1-y)^2} - \frac{27}{4} T_2 \right) = \alpha^2. \quad (6.5.1)$$

We list the critical temperature for some values of the coupling strength.

$$\alpha^2 = 507, \quad T_{cr} = 340$$

$$\alpha^2 = 50, \quad T_{cr} = 295.7$$

$$\alpha^2 = 40, \quad T_{cr} = 294.6$$

$$\alpha^2 = 30, \quad T_{cr} = 293.5$$

$$\alpha^2 = 20, \quad T_{cr} = 292.3$$

$$\alpha^2 = 8.5, \quad T_{cr} = 291$$

These values are taken from a graph, more accurate values can be obtained digitally, for example, at $\alpha^2 = 50$, $T_{cr} = 295.686$. From now on this is the value of α that have been used. The associated value of the normalised densities are 1/3; this gives the exact expression

$$T_{cr} = \frac{T_1 + T_2}{2} + \sqrt{\left(\frac{4}{27}\right)^2 \alpha^2 T_1 T_2 + \left(\frac{T_1 - T_2}{2}\right)^2}. \quad (6.5.2)$$

For $\alpha^2 = 50$ it gives $T_{cr} = 295.686$, both Mathematica (File Untitled-2) and Graphing Calculator.

The densities are molar, so \mathcal{R} is the universal gas constant.

I calculated the spinodal for $\alpha^2 = 50$ and temperatures ranging from 292.5K to 150K. As expected, the spinodal oval exists for $T \leq 295K$ and reaches the vertical axis when $T = 289.8K$.

Again as expected, each pair of coexistent densities bracket the spinodal at a distance is nearly constant except when the isobar is tangent to the spinodal; these are the configurations that are labelled “critical” in the sense of the experimenter. Confrontation with experiments makes it very clear

that this model is not realistic. The conclusion so far is that the interaction $\alpha\rho_1\rho_2$ does not give results that agree with experiments. I have done some calculations with the alternative interaction proportional to $\beta\sqrt{\rho_1\rho_2}$. but I have not gone further because of the dearth of measurements. there is ample support for the expectation expressed by some experimenter that the coordinates of the critical points are discontinuous as functions of the temperature.

Project 4. Collect all experimental data for one or more of the mixtures that are dealt with above. Make a detailed study of the success or lack of it of the interaction $\alpha\rho_1\rho_2 + \alpha'\sqrt{\rho_1\rho_2}$.